

Relaxation of Pseudo pure states : The Role of Cross-Correlations

Arindam Ghosh and Anil Kumar*

NMR Quantum Computation and Quantum Information Group

Department of Physics and Sophisticated Instruments Facility,

Indian Institute of Science, Bangalore-560012, India

In Quantum Information Processing by NMR one of the major challenges is relaxation or decoherence. Often it is found that the equilibrium mixed state of a spin system is not suitable as an initial state for computation and a definite initial state is required to be prepared prior to the computation. As these preferred initial states are non-equilibrium states, they are not stationary and are destroyed with time as the spin system relaxes toward its equilibrium, introducing error in computation. Since it is not possible to cut off the relaxation processes completely, attempts are going on to develop alternate strategies like Quantum Error Correction Codes or Noiseless Subsystems. Here we study the relaxation behavior of various Pseudo Pure States and analyze the role of Cross terms between different relaxation processes, known as Cross-correlation. It is found that while cross-correlations accelerate the relaxation of certain pseudo pure states, they retard that of others.

I. INTRODUCTION

Quantum information processing (QIP) often requires pure state as the initial state [1, 2]. Shor's prime factorizing algorithm [3], Grover search algorithm [4] are few examples. Creation of pure state in NMR is not easy due to small gaps between nuclear magnetic energy levels and demands unrealistic experimental conditions like near absolute zero temperature or extremely high magnetic field. This problem has been circumvented by creating a Pseudo Pure State (PPS). While in a pure state all energy levels except one have zero populations, in a PPS all levels except one have equal populations. Since the uniform background populations do not contribute to the NMR signal, such a state then mimics a pure state. Several methods of creating PPS have been developed like spatial averaging [5, 6], logical labeling [7, 8, 9, 10], temporal averaging [11], spatially averaged logical labeling technique (SALLT) [12]. However pseudo pure state, as well as pure states are not stationary and are destroyed with time as the spin system relaxes toward equilibrium. In QIP there are also cases where one or more qubits are initialized to a suitable state at the beginning of the computation

*DAE-BRNS Senior Scientist.; Electronic address: anilnmr@physics.iisc.ernet.in

and are used as storage or memory qubits at the end of the computation performed on some other qubits[13]. In these cases it is important for memory qubits to be in the initialized state till the time they are in use since deviation from the initial state adds error to the output result. Since it is not possible to stop decay of a state which is away from equilibrium, alternate strategies like Quantum Error Correction [14], Noiseless subspace [15, 16] are being tried. Recently Sarthour et al.[17] has reported a detailed study of relaxation of pseudo pure states and few other states in a quadrupolar system. Here we experimentally examine the lifetime of various pseudo pure states in a weakly J-coupled two qubit system. We find that cross terms (known as cross-correlation) between different pathways of relaxation of a spin can retard the relaxation of certain PPS and accelerate that of others.

In 1946 Bloch formulated the behavior of populations or longitudinal magnetizations when they are perturbed from the equilibrium [18]. The recovery toward equilibrium is exponential for a two level system and for a complex system the recovery involves several time constants [19]. For complex systems the von Neumann-Liouville equation [20, 21] describes mathematically the time evolution of the density matrix in the magnetic resonance phenomena. For system having more than one spin the relaxation is described by a matrix called the relaxation matrix whose elements are linear combinations of spectral densities, which in turn are Fourier transforms of time correlation function [22] of the fluctuations of the various interactions responsible for relaxation. There exist several different mechanisms for relaxation, such as, time dependent dipole-dipole(DD) interaction, chemical shift anisotropy(CSA), quadrupolar interaction and spin rotation interaction [22]. The correlation function gives the time correlations between different values of the interactions. The final correlation function has two major parts, namely the ‘Auto-correlation’ part which gives at two different times the correlation between the same relaxation interaction and the ‘Cross-correlation’ part which gives the time correlation between two different relaxation interactions. The mathematics of cross correlation can be found in detail, in works of Schneider [23, 24], Blicharski [25] and Hubbard [26]. Recently a few models have been suggested to study the decoherence of the quantum coherence, the off-diagonal elements in density matrix [27, 28]. It can be shown that in absence of r.f. pulses and under secular approximation the relaxation of the diagonal and the off-diagonal elements of the density matrix are independent [19]. Here we study the longitudinal relaxation that is the relaxation of the diagonal elements of the density matrix and the role of cross-correlations in it.

II. THEORY

A. The Pseudo Pure State (PPS) : In terms of magnetization modes

In terms of magnetization modes the equilibrium density matrix of a two spin system is given by [6, 21, 29, 30][Fig.1],

$$\chi_{eq} = \gamma_1 I_{1Z} + \gamma_2 I_{2Z} \quad (1)$$

where γ_1 and γ_2 are gyro-magnetic ratios of the two spins I_1 and I_2 respectively. The density matrix of a general state can be written as,

$$\chi = \pm\alpha\gamma_1 I_{1Z} \pm \beta\gamma_2 I_{2Z} \pm \nu\gamma_1 2I_{1Z}I_{2Z} \quad (2)$$

which for the condition $\alpha\gamma_1=\beta\gamma_2=\nu\gamma_1=K$, corresponds to the density matrix of a PPS given by [6],

$$\chi_{pps} = K[\pm I_{1Z} \pm I_{2Z} \pm 2I_{1Z}I_{2Z}] \quad (3)$$

where, K is a constant, the value of which depends on the method of creation of PPS.

The first two terms in the right hand side in Eq.2 and Eq.3 are the single spin order modes for the first and second spin respectively while the last term is the two spin order mode of the two spins [6].

Choosing properly the signs of the modes, the various PPS of a two-qubit system are,

$$\begin{aligned} \chi_{pps}^{00} &= K[+I_{1Z} + I_{2Z} + 2I_{1Z}I_{2Z}] \\ \chi_{pps}^{01} &= K[-I_{1Z} + I_{2Z} + 2I_{1Z}I_{2Z}] \\ \chi_{pps}^{10} &= K[+I_{1Z} - I_{2Z} + 2I_{1Z}I_{2Z}] \\ \chi_{pps}^{11} &= K[+I_{1Z} + I_{2Z} - 2I_{1Z}I_{2Z}] \end{aligned} \quad (4)$$

The relative populations of the states for different PPS are shown in Fig. 2. As seen in Eq.2, in PPS the coefficients of the all three modes are equal. On the other hand equilibrium density matrix does not contain any two spin order mode. To reach Eq.3 starting from Eq.1, the two spin order mode has to be created and at the same time the coefficients of all the modes have to be made equal.

B. Relaxation of Magnetization Modes

The equation of motion of modes M is given by [22],

$$-\frac{d}{dt}\vec{M}(t) = \hat{\Gamma}[\vec{M}(t) - \vec{M}(\infty)] \quad (5)$$

where $\hat{\Gamma}$ is the relaxation matrix and $\vec{M}(\infty)$ is the equilibrium values of a mode. For a weakly coupled two-spin system relaxing via mutual dipolar interaction and the CSA relaxation, the two dominant mechanism of relaxation of spin half nuclei in liquid state, the above equation takes the form,

$$-\frac{d}{dt} \begin{bmatrix} I_{1Z}(t) \\ I_{2Z}(t) \\ 2I_{1Z}I_{2Z}(t) \end{bmatrix} = \begin{bmatrix} \rho_1 & \sigma_{12} & \delta_{1,12} \\ \sigma_{12} & \rho_2 & \delta_{2,12} \\ \delta_{1,12} & \delta_{2,12} & \rho_{12} \end{bmatrix} \cdot \begin{bmatrix} I_{1Z}(0) - I_{1Z}(\infty) \\ I_{2Z}(0) - I_{2Z}(\infty) \\ 2I_{1Z}I_{2Z} \end{bmatrix} \quad (6)$$

where ρ_i is the self relaxation rate of the single spin order mode of spin \mathbf{i} , ρ_{ij} is the self relaxation rate of the two spin order mode of spin \mathbf{i} and \mathbf{j} , σ_{ij} is the cross-relaxation (Nuclear Overhauser Effect, NOE) rate between spins \mathbf{i} and \mathbf{j} and $\delta_{i,ij}$ is the cross-correlation term between CSA relaxation of spin \mathbf{i} and the dipolar relaxation between the spins \mathbf{i} and \mathbf{j} . ρ and σ involve only the auto-correlation terms and δ involves only the cross-correlation terms[22]. Magnetization modes of one order relaxes to other orders through cross-correlation and in absence of it the relaxation matrix becomes block diagonal within each order. The relaxation of modes are in general dominated by their self relaxation ρ , but in case of samples having long T_1 , the cross-correlation terms become comparable with self-relaxation and play an important role in relaxation of the spins.

The formal solution of Eq. 5 is given by,

$$\vec{M}(t) = \vec{M}(\infty) + [\vec{M}(0) - \vec{M}(\infty)]\exp(-\hat{\Gamma}t) \quad (7)$$

As time evolution of various modes are coupled, a general solution of the above equation requires diagonalization of the relaxation matrix. However, in the initial rate approximation Eq.7 can be written (for small values of $t=\tau$) as,

$$\begin{aligned} \vec{M}(\tau) &= \vec{M}(\infty) + [\vec{M}(0) - \vec{M}(\infty)][1 - \hat{\Gamma}\tau] \\ &= \vec{M}(0) - \hat{\Gamma}\tau[\vec{M}(0) - \vec{M}(\infty)] \end{aligned} \quad (8)$$

This equation asserts that in the initial rate approximation (for low τ), the decay or growth of a mode is linear with time and the initial slope is proportional to the corresponding relaxation matrix element. If the modes are allowed to relax for a longer time, their decay or growth deviates from the linear nature and adopts a multi-exponential behavior to finally reach the equilibrium[22].

C. Relaxation of Pseudo pure state

Let a two qubit system be in $|00\rangle$ PPS at $t=0$.

$$\chi^{00}(0) = K[I_{1Z} + I_{2Z} + 2I_{1Z}I_{2Z}] \quad (9)$$

After time t it will relax to,

$$\chi^{00}(t) = (K + \Delta_1(t))I_{1Z} + (K + \Delta_2(t))I_{2Z} + (K + \Delta_{12}(t))2I_{1Z}I_{2Z} \quad (10)$$

where $\Delta_1(t), \Delta_2(t)$ and $\Delta_{12}(t)$ are the time dependent deviations of respective modes from their initial values. The deviation of the two spin order can be measured from spectrum of either spin. Eq.10 can also be written as,

$$\chi^{00}(t) = (K + \Delta_{12}(t))[I_{1Z} + I_{2Z} + 2I_{1Z}I_{2Z}] + (\Delta_1(t) - \Delta_{12}(t))I_{1Z} + (\Delta_2(t) - \Delta_{12}(t))I_{2Z} \quad (11)$$

The first term is the pseudo pure state with the coefficient decreasing in time while the other two terms are the excesses of the single spin order modes with coefficients increasing in time. For other pseudo pure states Eq.11 becomes,

$$\chi^{01}(t) = (K + \Delta_{12}(t))[-I_{1Z} + I_{2Z} + 2I_{1Z}I_{2Z}] + (\Delta_1(t) + \Delta_{12}(t))I_{1Z} + (\Delta_2(t) - \Delta_{12}(t))I_{2Z} \quad (12)$$

$$\chi^{10}(t) = (K + \Delta_{12}(t))[I_{1Z} - I_{2Z} + 2I_{1Z}I_{2Z}] + (\Delta_1(t) - \Delta_{12}(t))I_{1Z} + (\Delta_2(t) + \Delta_{12}(t))I_{2Z} \quad (13)$$

$$\chi^{11}(t) = (K - \Delta_{12}(t))[I_{1Z} + I_{2Z} - 2I_{1Z}I_{2Z}] + (\Delta_1(t) + \Delta_{12}(t))I_{1Z} + (\Delta_2(t) + \Delta_{12}(t))I_{2Z} \quad (14)$$

In the initial rate approximation (using Eq.8) we obtain for the $|00\rangle$ pps,

$$\Delta_1(\tau) = \tau[\rho_1(\gamma_1 - K) + \sigma_{12}(\gamma_2 - K) - K\delta_{1,12}] \quad (15)$$

$$\Delta_2(\tau) = \tau[\sigma_{12}(\gamma_1 - K) + \rho_1(\gamma_2 - K) - K\delta_{2,12}] \quad (16)$$

$$\Delta_{12}(\tau) = \tau[\delta_{1,12}(\gamma_1 - K) + \delta_{2,12}(\gamma_2 - K) - K\rho_{12}] \quad (17)$$

Let the coefficients of the PPS term and the two single spin order modes I_{1Z} and I_{2Z} in Eq.11 be called as \mathcal{A}, \mathcal{B} and \mathcal{C} respectively. Fig.3 schematically shows the time evolution of the coefficients \mathcal{A}, \mathcal{B} and \mathcal{C} for $|00\rangle$ PPS. Any coefficient for any PPS at any instant, is simply the initial value plus the total deviation due to the auto and the cross-correlations. For example, \mathcal{A} for $|00\rangle$ PPS at time τ , is $\mathcal{A}^{00}(\tau) = K + \mathcal{A}_{auto}^{00}(\tau) + \mathcal{A}_{cc}^{00}(\tau)$, where K is the initial value, and $\mathcal{A}_{auto}^{00}(\tau)$ and $\mathcal{A}_{cc}^{00}(\tau)$ are the deviations at τ due to auto-correlation and cross-correlation parts respectively.

(a) Contribution of auto-correlation terms to the deviation

Putting the values of the deviations of different modes obtained from Eq.(15-17) in Eq.(11-14), we obtain the contribution only of auto-correlation terms to the deviation from initial value of the coefficients \mathcal{A}, \mathcal{B} and \mathcal{C} under initial rate approximation (at $t=\tau$) as,

$$\begin{aligned}\mathcal{A}_{auto}^{00}(\tau) &= \mathcal{A}_{auto}^{01}(\tau) = \mathcal{A}_{auto}^{10}(\tau) = \mathcal{A}_{auto}^{11}(\tau) = -K\rho_{12}\tau \\ \mathcal{B}_{auto}^{00}(\tau) &= [\rho_1(\gamma_1 - K) + \sigma_{12}(\gamma_2 - K) + K\rho_{12}]\tau ; \mathcal{B}_{auto}^{01}(\tau) = [\rho_1(\gamma_1 + K) + \sigma_{12}(\gamma_2 - K) - K\rho_{12}]\tau \\ \mathcal{B}_{auto}^{10}(\tau) &= [\rho_1(\gamma_1 - K) + \sigma_{12}(\gamma_2 + K) + K\rho_{12}]\tau ; \mathcal{B}_{auto}^{11}(\tau) = [\rho_1(\gamma_1 - K) + \sigma_{12}(\gamma_2 - K) + K\rho_{12}]\tau \\ \mathcal{C}_{auto}^{00}(\tau) &= [\sigma_{12}(\gamma_1 - K) + \rho_2(\gamma_2 - K) + K\rho_{12}]\tau ; \mathcal{C}_{auto}^{01}(\tau) = [\sigma_{12}(\gamma_1 + K) + \rho_2(\gamma_2 - K) + K\rho_{12}]\tau \\ \mathcal{C}_{auto}^{10}(\tau) &= [\sigma_{12}(\gamma_1 - K) + \rho_2(\gamma_2 + K) - K\rho_{12}]\tau ; \mathcal{C}_{auto}^{11}(\tau) = [\sigma_{12}(\gamma_1 - K) + \rho_2(\gamma_2 - K) + K\rho_{12}]\tau\end{aligned}\quad (18)$$

It is evident that in absence of cross-correlations the $|00\rangle$ and $|11\rangle$ PPS relax at the same initial rate since $\mathcal{A}_{auto}^{00} = \mathcal{A}_{auto}^{11}$, $\mathcal{B}_{auto}^{00} = \mathcal{B}_{auto}^{11}$ and $\mathcal{C}_{auto}^{00} = \mathcal{C}_{auto}^{11}$. However the same is not true for $|01\rangle$ and $|10\rangle$ PPS.

(b) Contribution of cross-correlation terms to the deviation

The contribution by the cross-correlation terms is given by,

$$\begin{aligned}\mathcal{A}_{cc}^{00}(\tau) &= +[\delta_{1,12}(\gamma_1 - K) + \delta_{2,12}(\gamma_2 - K)]\tau \\ \mathcal{A}_{cc}^{01}(\tau) &= +[\delta_{1,12}(\gamma_1 + K) + \delta_{2,12}(\gamma_2 - K)]\tau \\ \mathcal{A}_{cc}^{10}(\tau) &= +[\delta_{1,12}(\gamma_1 - K) + \delta_{2,12}(\gamma_2 + K)]\tau \\ \mathcal{A}_{cc}^{11}(\tau) &= -[\delta_{1,12}(\gamma_1 - K) + \delta_{2,12}(\gamma_2 - K)]\tau \\ \mathcal{B}_{cc}^{00}(\tau) &= -[\delta_{1,12}\gamma_1 + \delta_{2,12}(\gamma_2 - K)]\tau ; \mathcal{B}_{cc}^{01}(\tau) = +[\delta_{1,12}\gamma_1 + \delta_{2,12}(\gamma_2 - K)]\tau \\ \mathcal{B}_{cc}^{10}(\tau) &= -[\delta_{1,12}\gamma_1 + \delta_{2,12}(\gamma_2 + K)]\tau ; \mathcal{B}_{cc}^{11}(\tau) = +[\delta_{1,12}\gamma_1 + \delta_{2,12}(\gamma_2 - K)]\tau \\ \mathcal{C}_{cc}^{00}(\tau) &= -[\delta_{1,12}(\gamma_1 - K) + \delta_{2,12}\gamma_2]\tau ; \mathcal{C}_{cc}^{01}(\tau) = -[\delta_{1,12}(\gamma_1 + K) + \delta_{2,12}\gamma_2]\tau \\ \mathcal{C}_{cc}^{10}(\tau) &= +[\delta_{1,12}(\gamma_1 - K) + \delta_{2,12}\gamma_2]\tau ; \mathcal{C}_{cc}^{11}(\tau) = +[\delta_{1,12}(\gamma_1 - K) + \delta_{2,12}\gamma_2]\tau\end{aligned}\quad (19)$$

The important thing is that the presence of cross-correlation can lead to differential relaxation of all PPS. Positive cross-correlation rates $\delta_{1,12}$ and $\delta_{2,12}$, slow down the relaxation of all the three coefficients for $|00\rangle$ PPS since ($\mathcal{A}^{00}(\tau) > \mathcal{A}_{auto}^{00}(\tau), \mathcal{B}^{00}(\tau) < \mathcal{B}_{auto}^{00}(\tau), \mathcal{C}^{00}(\tau) < \mathcal{C}_{auto}^{00}(\tau)$), while make the relaxation of all three coefficients faster for $|11\rangle$ PPS since ($\mathcal{A}^{11}(\tau) < \mathcal{A}_{auto}^{11}(\tau), \mathcal{B}^{11}(\tau) > \mathcal{B}_{auto}^{11}(\tau), \mathcal{C}^{11}(\tau) > \mathcal{C}_{auto}^{11}(\tau)$). For $|01\rangle$ and $|10\rangle$ PPS cross-correlations

give a mixed effect since ($\mathcal{A}^{01}(\tau) > \mathcal{A}_{auto}^{01}(\tau)$, $\mathcal{B}^{01}(\tau) > \mathcal{B}_{auto}^{01}(\tau)$, $\mathcal{C}^{01}(\tau) < \mathcal{C}_{auto}^{01}(\tau)$) and ($\mathcal{A}^{10}(\tau) > \mathcal{A}_{auto}^{00}(\tau)$, $\mathcal{B}^{10}(\tau) < \mathcal{B}_{auto}^{10}(\tau)$, $\mathcal{C}^{10}(\tau) > \mathcal{C}_{auto}^{10}(\tau)$). As the contributions of the auto-correlation part for $|00\rangle$ and $|11\rangle$ PPS are equal, we have monitored the relaxation behavior only of $|00\rangle$ and $|11\rangle$ PPS to study the effect of cross-correlations.

For samples having long T_1 , where the cross-correlations becomes comparable with auto-correlation rates, the four PPS relax with four different rates and the difference increases with the increased value of the cross-correlation terms. The three coefficients \mathcal{A} , \mathcal{B} and \mathcal{C} (normalized to the equilibrium line intensities) in terms of proton and fluorine line intensities for $|00\rangle$ PPS are,

$$\begin{aligned}\mathcal{A}(t) &= \frac{H^0(t) - H^1(t)}{H^1(\infty) + H^0(\infty)} = \frac{F^0(t) - F^1(t)}{F^1(\infty) + F^0(\infty)} \\ \mathcal{B}(t) &= \frac{2H^1(t)}{H^0(\infty) + H^1(\infty)} \\ \mathcal{C}(t) &= \frac{2F^1(t)}{F^0(\infty) + F^1(\infty)}\end{aligned}\tag{20}$$

and for $|11\rangle$ PPS are,

$$\begin{aligned}\mathcal{A}(t) &= \frac{H^1(t) - H^0(t)}{H^1(\infty) + H^0(\infty)} = \frac{F^1(t) - F^0(t)}{F^1(\infty) + F^0(\infty)} \\ \mathcal{B}(t) &= \frac{2H^0(t)}{H^0(\infty) + H^1(\infty)} \\ \mathcal{C}(t) &= \frac{2F^0(t)}{F^0(\infty) + F^1(\infty)}\end{aligned}\tag{21}$$

where, H^0 and H^1 are intensities of the two proton transitions, when the fluorine spin is respectively in state $|0\rangle$ and $|1\rangle$. Similarly F^0 and F^1 are intensities of two fluorine transitions corresponding to the proton spin being respectively in the state $|0\rangle$ and $|1\rangle$, as shown in Fig.1 and Fig.6. $H^0(t)$ and $H^0(\infty)$ give the H^0 line intensity respectively at time t and at equilibrium. Thus by monitoring the intensities of the two proton and two fluorine transitions as a function of time, one can calculate the coefficient $\mathcal{A}(t)$ which is a measure of decay of PPS.

III. SIMULATION

Relaxation of the coefficients \mathcal{A} , \mathcal{B} and \mathcal{C} have been simulated using MATLAB, for a weakly coupled $^{19}\text{F}-^1\text{H}$ system. The relaxation matrix used for the simulation is,

$$\hat{\Gamma} = \begin{bmatrix} 0.3125 & 0.02 & \delta_{1,12} \\ 0.02 & 0.33 & \delta_{2,12} \\ \delta_{1,12} & \delta_{2,12} & 0.33 \end{bmatrix}$$

Fig.4 shows the decay of coefficient \mathcal{A} with time. \mathcal{A}^{00} and \mathcal{A}^{11} show no difference in decay rate in absence of cross-correlation rates. As $\delta_{1,12}$ and $\delta_{2,12}$ are increased more and more difference in decay rate is observed. Fig.5 shows growth of coefficients \mathcal{B} and \mathcal{C} . As $\delta_{2,12}$ is taken smaller than $\delta_{1,12}$, difference in decay rate between \mathcal{C}^{00} and \mathcal{C}^{11} is found to be less than between \mathcal{B}^{00} and \mathcal{B}^{11} .

IV. EXPERIMENTAL

All the relaxation measurement were performed on a two qubit sample formed by one fluorine and one proton of 5-fluoro 1,3-dimethyl uracil yielding an AX spin system with a J-coupling of 5.8 Hz. Longitudinal relaxation time constants for ^{19}F and ^1H are 6 and 7.2 Sec respectively at room temperature (300K). All the experiments were performed in a Bruker DRX 500 MHz spectrometer where the resonance frequencies for ^{19}F and ^1H are 470.59 MHz and 500.13 MHz respectively. The Pseudo-pure state was prepared by spatial averaging method using J-evolution [6]. Relaxation of all the three coefficients for $|00\rangle$ and $|11\rangle$ PPS has been calculated. Since auto-correlations contribute equally to the relaxation of these two PPS, any difference in relaxation rate can be attributed to cross-correlation rates.

Sample temperature was varied to change the correlation time and hence the cross-correlation rate δ . Four different sample temperatures, 300K, 283K, 263K and 253K were used. Fig.6 shows the proton and fluorine spectra obtained using recovery measurement at four different temperatures. The spectra correspond to the initial PPS state and that after an interval of 2.5 sec. Fig.7 shows the longitudinal relaxation times (T_1) of fluorine and proton as function of temperature obtained from initial part of inversion-recovery experiment. A steady decrease in T_1 with decreasing temperature indicates that the dynamics of the sample molecule is in the short correlation time limit [21]. In this limit auto as well as cross-correlations increase linearly with decreasing temperature.

All the spectra were fitted to bi-Lorentzian lines in MATLAB and various parameters were extracted using the Origin software. Fig.8 shows the decay of the coefficient \mathcal{A} calculated independently from proton and fluorine spectra. At 300K, \mathcal{A}^{00} and \mathcal{A}^{11} showed almost same rate of decay. As the temperature was gradually lowered, a steady increase in difference in decay rate was observed. This is due to the steady increase in cross-correlation rates with decreasing temperature, which is expected in the short correlation time limit. In Fig.9 the growths of the coefficients \mathcal{B} and \mathcal{C} are shown. Similar to the coefficient \mathcal{A} , coefficients \mathcal{B} and \mathcal{C} also show differences in decay rate between $|00\rangle$ and $|11\rangle$ PPS at lower temperatures. The difference between \mathcal{B}^{00} and \mathcal{B}^{11} at any temperature was found to be larger compared to between \mathcal{C}^{00} and \mathcal{C}^{11} . This is expected since, according to Eq.19 the dominant cross-correlation factor in \mathcal{B}^{00} and \mathcal{B}^{11} is $\delta_{1,12}$ which is the cross-correlation between CSA of fluorine with fluorine-proton dipolar interaction whereas in \mathcal{C}^{00} and \mathcal{C}^{11} the dominant factor is $\delta_{2,12}$ which is cross-correlation between CSA of proton, which is much less than fluorine, with fluorine-proton dipolar interaction. Thus it is found that at lower temperatures the $|00\rangle$ PPS decays slower than the $|11\rangle$ PPS. The dominant difference in the decay rates arises from the cross-correlations between the CSA of the fluorine and the dipolar interaction between the fluorine and the proton spin. To the best of our knowledge this is the first study of its kind where the differential decay of the PPS has been attributed to cross-correlations.

V. CONCLUSION

We have demonstrated here that in samples having long T_1 cross-correlations plays an important role in determining the rate of relaxation of pseudo pure state. In QIP sometimes one or more qubits having comparatively longer longitudinal relaxation are used as storage or memory qubits. Recently Levitt et al. have demonstrated a long living antisymmetric state arrived by shifting the sample from high to very low magnetic field, suggesting that this long living state could be used as memory qubit [31, 32]. In such cases fidelity of computation depends on how much the memory qubits have been deviated from the initialized state at the beginning of the computation till the time they are actually used. Theoretically it is shown here that in presence of cross-correlations, all the four PPS relax with different initial rates. For positive cross-correlations the $|00\rangle$ PPS relaxes significantly slower than $|11\rangle$ PPS. It is therefore important to choose a proper initial pseudo pure state according to the sample.

Acknowledgments

We gratefully acknowledge Prof. K. V. Ramanathan for discussions and Mr. Rangeet Bhattacharyya for his help in data processing. The use of DRX-500 high resolution liquid state spectrometer of the Sophisticated Instrument Facility, Indian Institute of Science, Bangalore, funded by Department of Science and Technology (DST), New Delhi, is gratefully acknowledged. AK acknowledges "DAE-BRNS" for "Senior Scientist scheme", and DST for a research grant.

FIGURE CAPTIONS

Figure 1. (a) Chemical structure of 5-fluoro 1,3-dimethyl uracil. The fluorine and the proton spins (shown by circles) are used as the two qubits I_1 and I_2 respectively. (b) The energy level diagram of a two qubit system identifying the four states 00,01,10 and 11. Under high temperature and high field approximation [21] the relative equilibrium deviation populations are indicated in the bracket for each level. Assuming this to be a weakly coupled two spin system the deviation populations become proportional to the gyromagnetic ratios γ_1 and γ_2 . I_j^k refers to the transition of the j^{th} spin when the other spin is in state $|k\rangle$. Thus H^0 means the proton transition when the fluorine is in state $|0\rangle$.

Figure 2. Population distribution of different energy levels of a two spin system in different pseudo-pure states. K is a constant whose value depends on the protocol used for the preparation of PPS. (a),(b),(c) and (d) show respectively the $|00\rangle, |01\rangle, |10\rangle$ and $|11\rangle$ PPS.

Figure 3. Schematic representation of decay of the coefficient \mathcal{A} and growth of the coefficients \mathcal{B} and \mathcal{C} . The magnetization modes are normalized to their respective equilibrium values. In each sub-figure the three bars correspond to the modes I_{1Z}, I_{2Z} and $2I_{1Z}I_{2Z}$ from left to right. The amount of any mode present at any time is directly proportional to the height of the corresponding bar. The numbers provided in the rightmost column represent typical values of the modes. (a) Thermal equilibrium. At thermal equilibrium only I_{1Z} and I_{2Z} exist. (b) $|00\rangle$ pseudo-pure state just after creation, where all the three modes are equal in magnitude. For $|00\rangle$ PPS all modes are of same sign but this is not the case for other PPS [Eq.3]. Coefficient \mathcal{A} is the common equal amount of all the modes and it is maximum at $t=0$. (c) The amount of magnetization modes (schematic) at time τ , after preparation of the PPS at $t=0$. The two single spin order modes increase and the two spin order mode decreases from their initial values. (d) The state of various modes at time τ , (same as fig.c) redrawn with filled bar to indicate the residual value of \mathcal{A} . All the three coefficients \mathcal{A}, \mathcal{B} and \mathcal{C} are shown. \mathcal{A} (shown by the filled bar), which is the measure of the PPS, has come down by the same amount as the two spin order. \mathcal{B} (shown by the empty bar) and \mathcal{C} (shown by the striped bar) are the residual part of the single spin order modes I_{1Z} and I_{2Z} respectively. (e) The values of various modes and coefficients after a delay $\tau' > \tau$.

Figure 4. Simulation of decay of coefficient \mathcal{A} . The boxes (\square) and circles (\circ) correspond to

the $|11\rangle$ and $|00\rangle$ PPS respectively. In each plot deviation from initial value ($\mathcal{A}(t) - \mathcal{A}(0)$) has been plotted.

Figure 5. Simulation of growth of coefficient \mathcal{B} and \mathcal{C} . The boxes (\square) and circles (\circ) correspond to the $|11\rangle$ and $|00\rangle$ PPS respectively.

Figure 6. Relaxation of Pseudo pure state as monitored on (a) fluorine spin and (b) proton spin of the 5-fluoro 1,3-dimethyl uracil at four different temperatures. The top row in (a) and (b) show the equilibrium spectrum at each temperature. With decrease in temperatures the lines broaden due to decreased T_2 . The second row in (a) and (b) show the spectra corresponding to the $|00\rangle$ PPS, prepared by spatial averaging method using J-evolution. The state of PPS was measured by 90° pulse at each spin. The third row in (a) and (b) show the spectra after an interval of 2.5 seconds after creation of the $|00\rangle$ PPS. The fourth row shows the spectra immediately after creation of $|11\rangle$ PPS and the fifth row, the spectra after 2.5 seconds.

Figure 7. Longitudinal relaxation time T_1 of fluorine (a) and proton (b) as function of temperature, measured from the initial part of inversion recovery experiment for each spin.

Figure 8. The deviation from initial value (at $t=0$) of the coefficient \mathcal{A} of the PPS term calculated from Proton (left column) and Fluorine (right column) at four different sample temperature. The empty (\circ) and filled (\bullet) circles correspond to the $|00\rangle$ and $|11\rangle$ PPS respectively.

Figure 9. The growth of the coefficients \mathcal{B} and \mathcal{C} at different sample temperatures. \mathcal{B} was calculated from Fluorine spectrum while \mathcal{C} was calculated from the Proton spectrum. The empty (\circ) and filled (\bullet) circles correspond to the $|00\rangle$ and $|11\rangle$ PPS respectively.

-
- [1] J. Preskill, Lecture notes for Physics 229: Quantum information and Computation, <http://theory.caltech.edu/people/preskill/>.
 - [2] M.A. Nielsen and I.L. Chuang, Quantum Computation and Quantum Information, Cambridge University Press 2000.
 - [3] P.W. Shor, Polynomial-time algorithms for prime factorization and discrete algorithms on quantum computer, SIAM Rev. 41 (1999) 303-332.
 - [4] L.K. Grover, Quantum Mechanics helps in searching for a needle in a haystack, Phys. Rev. Lett. 79 (1997) 325.
 - [5] D.G. Cory, A.F. Fahmy and T.F. Havel, Ensemble quantum computing by NMR spectroscopy, Proc. Natl. Acad. Sci. USA, 94 (1997) 1634.
 - [6] D.G. Cory, M. D. Price and T.F. Havel, Nuclear magnetic resonance spectroscopy: An experimentally accessible paradigm for quantum computing, Physica D, 120 (1998) 82.
 - [7] N. Gershenfeld and I.L. Chuang, Bulk spin-resonance quantum computation, Science, 275 (1997) 350.
 - [8] I.L. Chuang, N. Gershenfeld, M.G. Kubines and D.W. Leung, Bulk quantum computation with nuclear magnetic resonance, Proc. Roy. Soc. Lond. A, 454 (1998) 447-467.
 - [9] Kavita Dorai, Arvind and Anil Kumar, Implementing quantum-logic operations, pseudopure states, and the Deutsch-Jozsa algorithm using noncommuting selective pulses in NMR, Phys. Rev. A. 61 (2000) 042306.
 - [10] Kavita Dorai, T.S. Mahesh, Arvind and Anil Kumar, Quantum Computations by NMR, Current Science. 79 (2000) 1447-1458.
 - [11] E. Knill, I. L. Chuang and R. Laflamme, Effective pure states for bulk quantum computation, Phys. Rev. A. 57 (2000) 3348.
 - [12] T.S. Mahesh and Anil Kumar, Ensemble quantum-information processing by NMR: Spatially averaged logical labeling technique for creating pseudopure states, Phys. Rev. A. 64 (2001) 012307.
 - [13] D. Gottesman and I.L. Chuang, Demonstrating the viability of universal quantum computation using teleportation and single-qubit operations, Nature (London). 402 (1999) 390.
 - [14] E. Knill and R. Laflamme, Theory of quantum error correcting codes, Phys. Rev. A. 55 (1997) 900-911.
 - [15] E. Knill, R. Laflamme and L. Viola, Theory of Quantum Error Correction for General Noise, Phys. Rev. Lett. 84 (2000) 2525.
 - [16] L. Viola, E. M. Fortunato, M. A. Pravia, E. Knill, R. Laflamme and D. G. Cory, Experimental realization of Noiseless Subsystems for Quantum Information Processing, Science. 293 (2001) 2059-2063.
 - [17] R. S. Sarthour, E. R. deAzevedo, F. A. Bonk, E. L. G. Vidoto, T. J. Bonagamba, A. P. Guimarães, J. C. C. Freitas and I. S. Oliveira, Relaxation of coherent states in a two-qubit NMR quadrupolar system, Phys. Rev. A. 68 (2003) 022311.
 - [18] F. Bloch, Nuclear Induction, Phys. Rev. 70 (1946) 460.
 - [19] A. G. Redfield, The theory of relaxation processes, Adv. Mag. Res. 1 (1966) 1.
 - [20] J. von Neumann, Measurement and reversibility and The measuring process, chapter V and VI in Mathematische Grundlagen der Quantenmechanik, Springer, Berlin (1932). English translation by R. T. Beyer, Mathematical Foundations of Quantum Mechanics, Princeton Univ. Press, Princeton.
 - [21] A. Abragam, Principles of Nuclear Magnetic Resonance, Clarendon Press, Oxford, 1961.
 - [22] Anil Kumar, R. C. R. Grace, P. K. Madhu, Cross Correlation in NMR, Prog. in Nucl. Mag. Res. Spec. 37 (2000) 191-319.
 - [23] H. Schneider, Kernmagnetische Relaxation von Drei-Spin-Molekülen im flüssigen oder adsorbierten Zustand. I, Ann. Phys. 13 (1964) 313.
 - [24] H. Schneider, Kernmagnetische Relaxation von Drei-Spin-Molekülen im flüssigen oder adsorbierten Zustand. II, Ann. Phys. 16 (1965) 135.

- [25] J. S. Blicharski, Interference effect in nuclear magnetic relaxation, Phys. Lett. 24 (1967) 608.
- [26] P. S. Hubbard, Some properties of Correlation functions of Irreducible Tensor Operators, Phys. Rev. 180 (1969) 319.
- [27] W. H. Zurek, Environment-induced superselection rules, Phys. Rev. D. 26 (1982) 1862.
- [28] G. Teklemariam, E. M. Fortunato, C. C. Lopez, J. Emerson, J. P. Paz, T. F. Havel and D. G. Cory, A Method for Modeling Decoherence on a Quantum Information Processor, Phys. Rev. A. 67 (2003) 062316.
- [29] R.R. Ernst, G. Bodenhausen, and A. Wokaun, Principles of Nuclear Magnetic Resonance in One and Two Dimensions, Clarendon press, Oxford, 1987.
- [30] J. A. Jones, R. H. Hansen and M. Mosca, Quantum Logic Gates and Nuclear Magnetic Resonance Pulse Sequences, J. of Mag. Res. 135 (1998) 353.
- [31] M. Carravetta and M. H. Levitt, Long-lived nuclear spin states in high-field solution NMR, J. Am. Chem. Soc. 126 (2004) 6228.
- [32] M. Carravetta, O. G. Johannessen and Malcolm H. Levitt, Beyond the T_1 Limit: Singlet Nuclear Spin States in Low Magnetic Fields, Phys. Rev. Lett. 92 (2004) 153003.

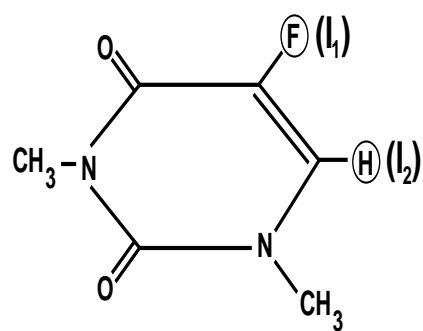
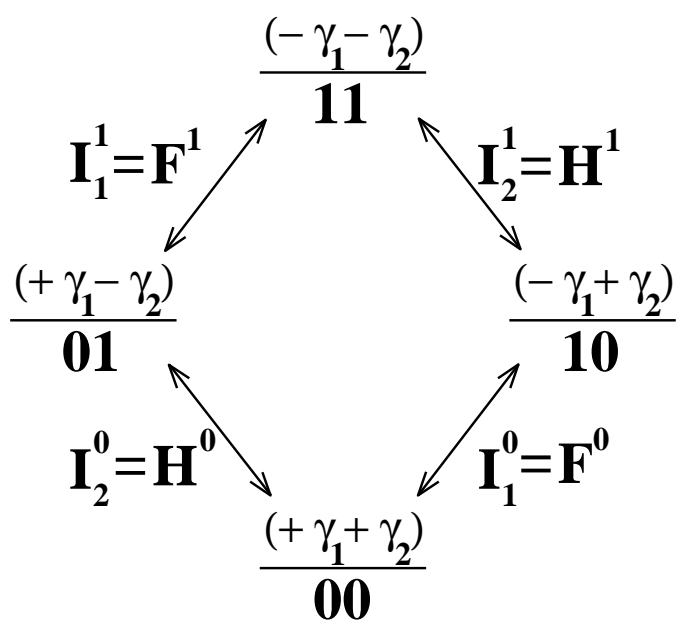
(a)**(b)**

Figure 1:

<div data-bbox="183 254 423 310">(a) $00\rangle$PPS</div> <div data-bbox="423 394 553 485">$\frac{-K/2}{11}$</div> <div data-bbox="245 575 370 665">$\frac{-K/2}{01}$</div> <div data-bbox="613 575 738 665">$\frac{-K/2}{10}$</div> <div data-bbox="423 756 553 846">$\frac{3K/2}{00}$</div>	<div data-bbox="779 254 1019 310">(b) $01\rangle$PPS</div> <div data-bbox="1019 394 1144 485">$\frac{K/2}{11}$</div> <div data-bbox="824 575 950 665">$\frac{-3K/2}{01}$</div> <div data-bbox="1193 575 1318 665">$\frac{K/2}{10}$</div> <div data-bbox="1019 756 1144 846">$\frac{K/2}{00}$</div>
<div data-bbox="183 924 423 980">(c) $10\rangle$PPS</div> <div data-bbox="423 1085 553 1176">$\frac{K/2}{11}$</div> <div data-bbox="245 1266 370 1356">$\frac{K/2}{01}$</div> <div data-bbox="613 1266 738 1356">$\frac{-3K/2}{10}$</div> <div data-bbox="423 1446 553 1537">$\frac{K/2}{00}$</div>	<div data-bbox="779 924 1019 980">(d) $11\rangle$PPS</div> <div data-bbox="1019 1085 1144 1176">$\frac{-3K/2}{11}$</div> <div data-bbox="824 1266 950 1356">$\frac{K/2}{01}$</div> <div data-bbox="1193 1266 1318 1356">$\frac{K/2}{10}$</div> <div data-bbox="1019 1446 1144 1537">$\frac{K/2}{00}$</div>

Figure 2:

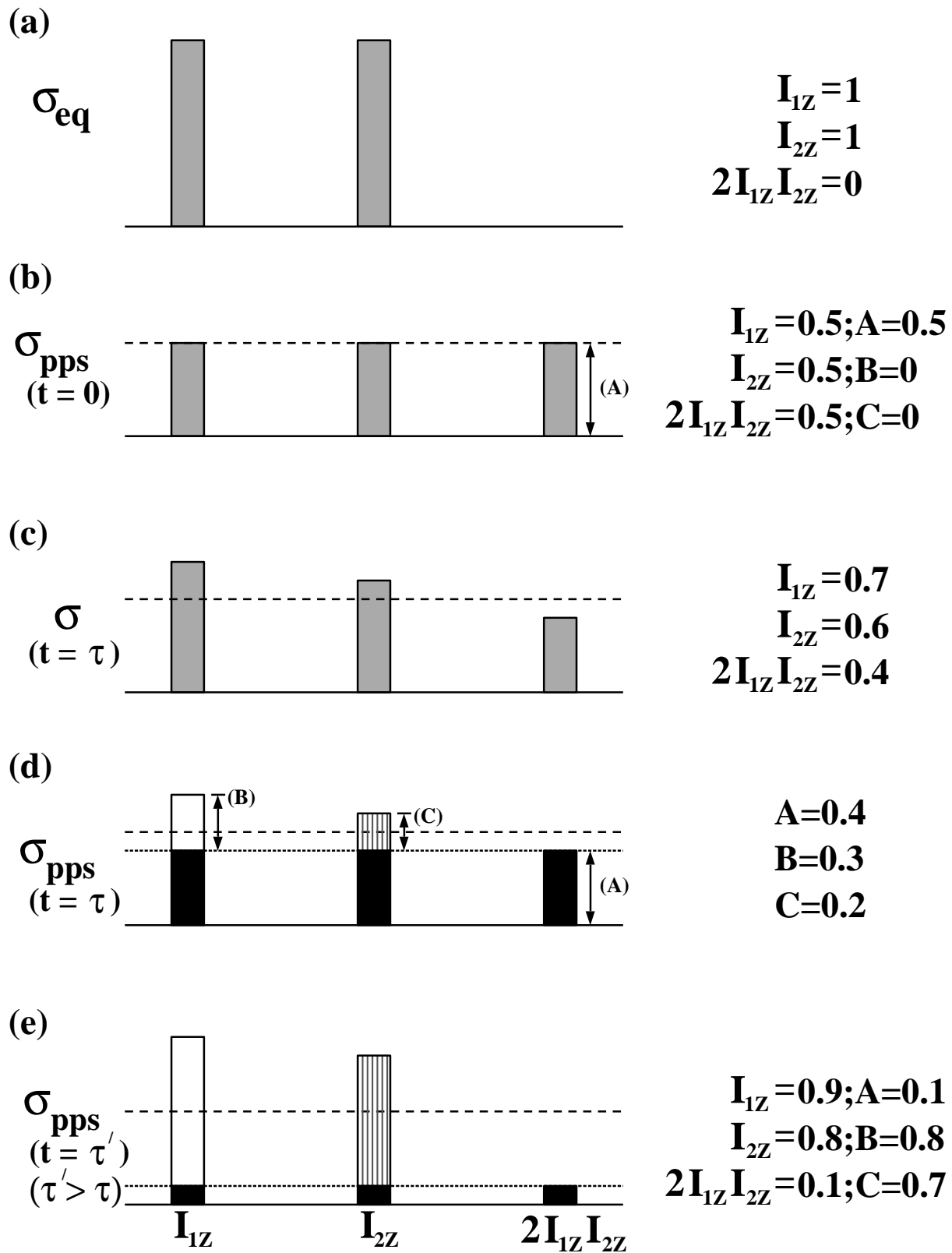


Figure 3:

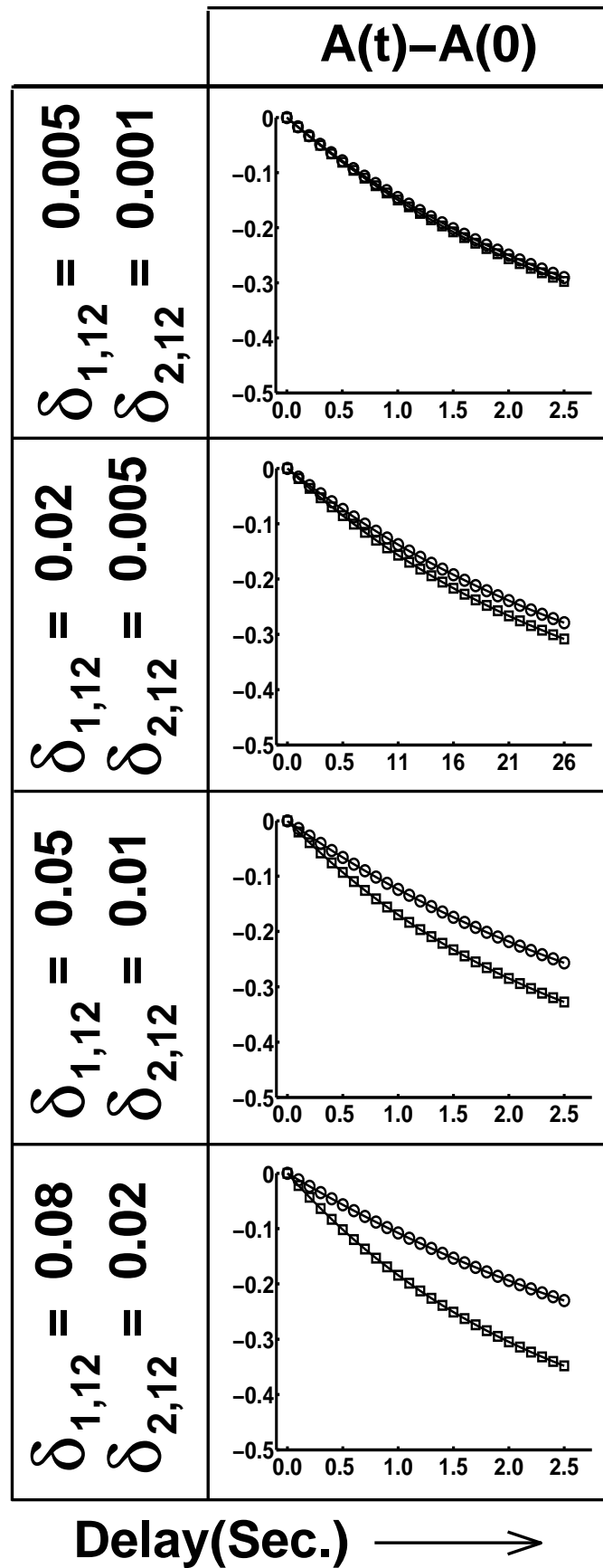


Figure 4:

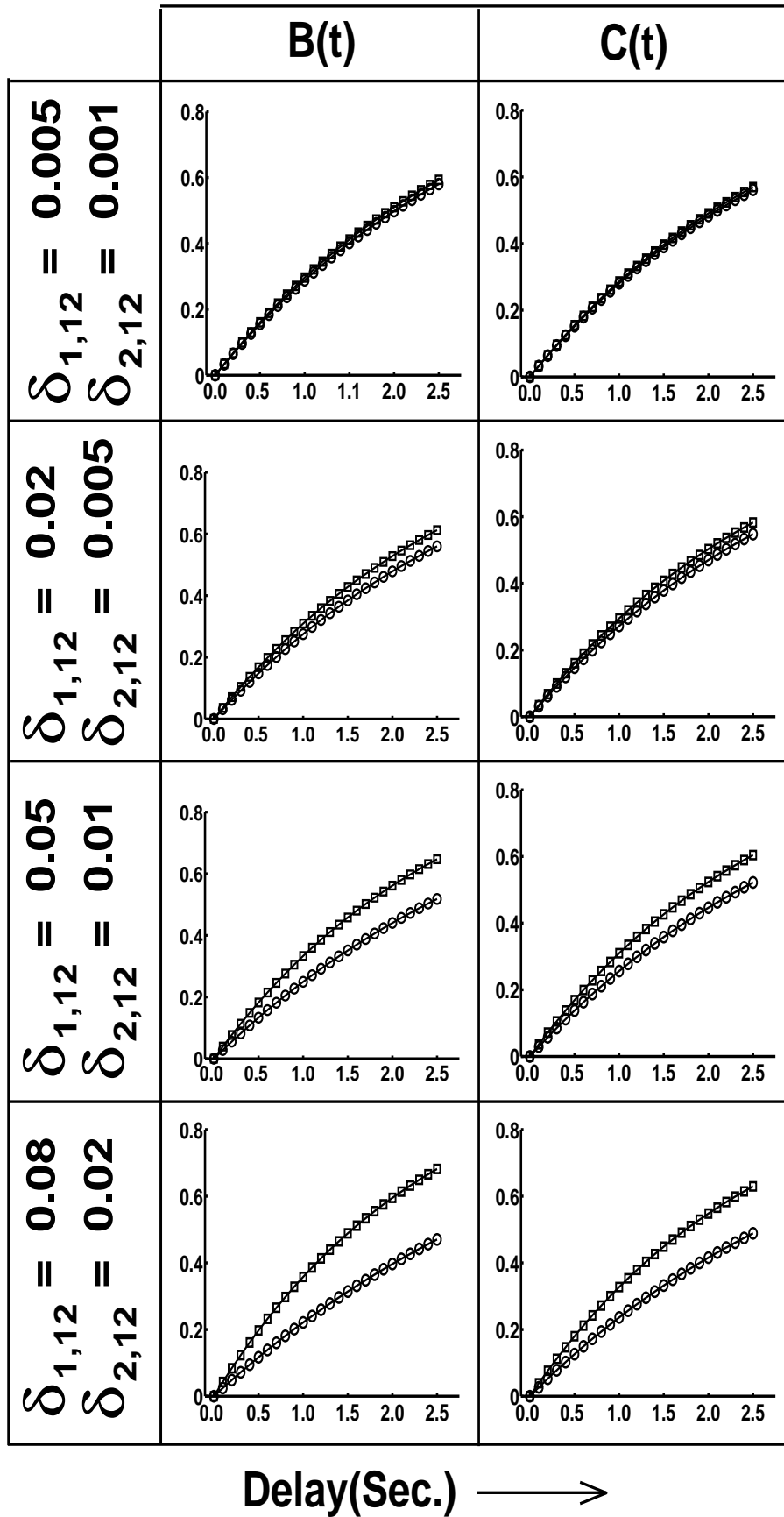


Figure 5:

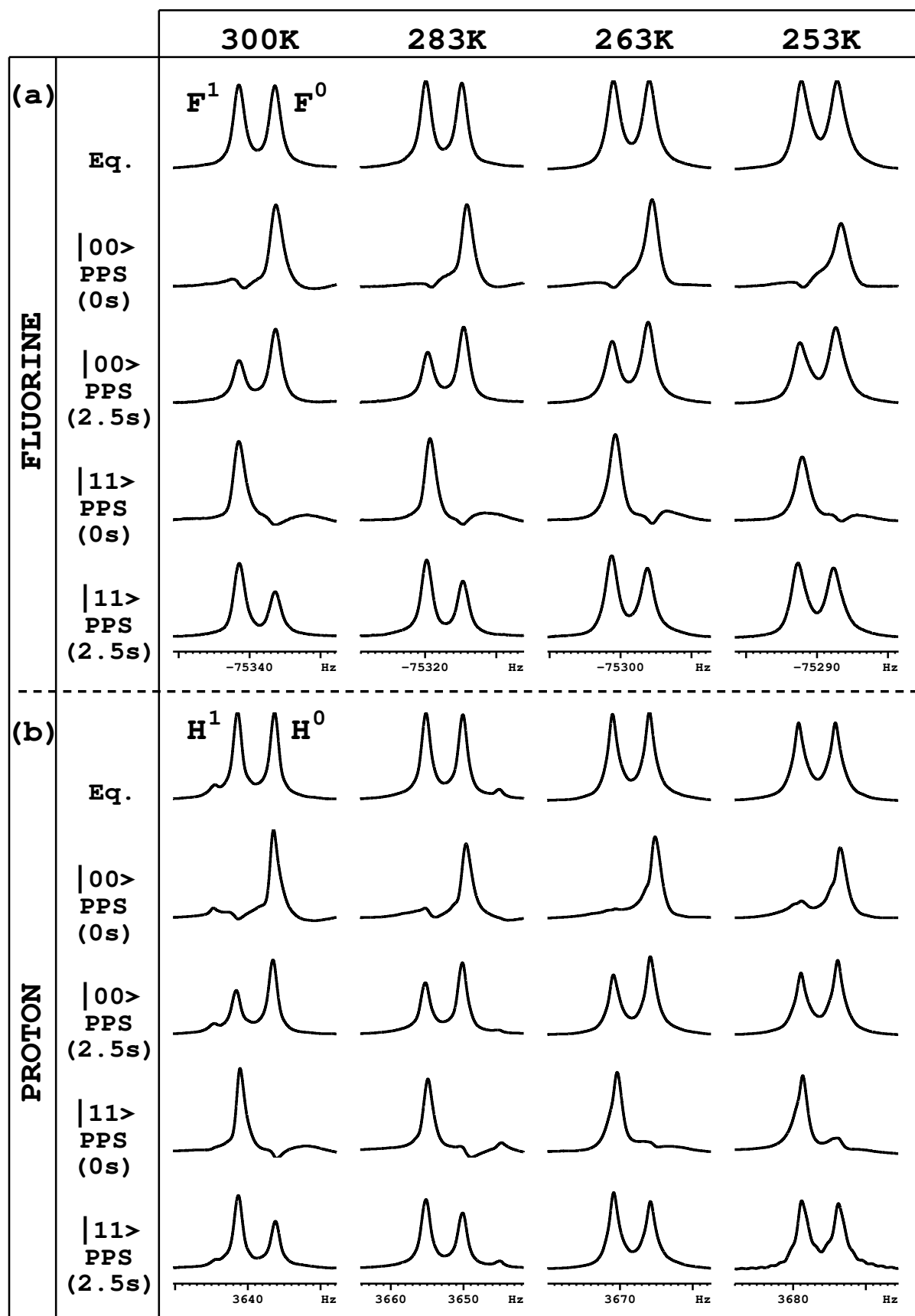


Figure 6:

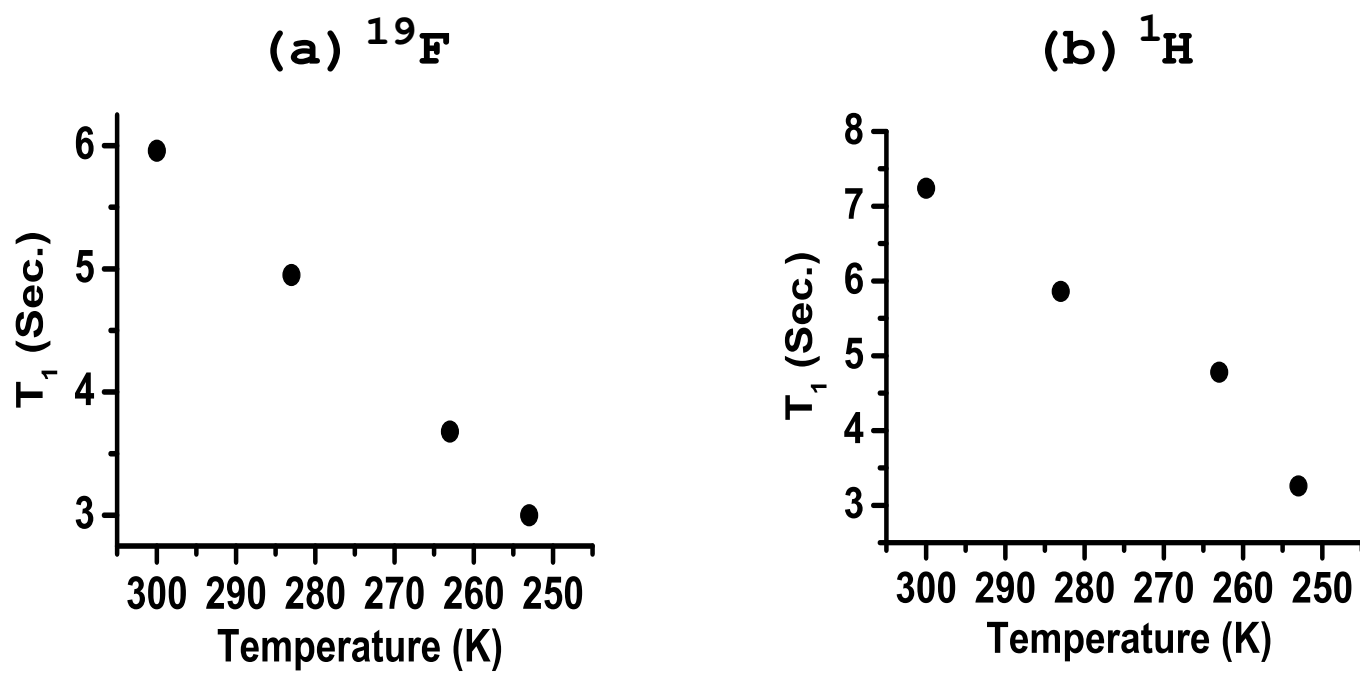


Figure 7:

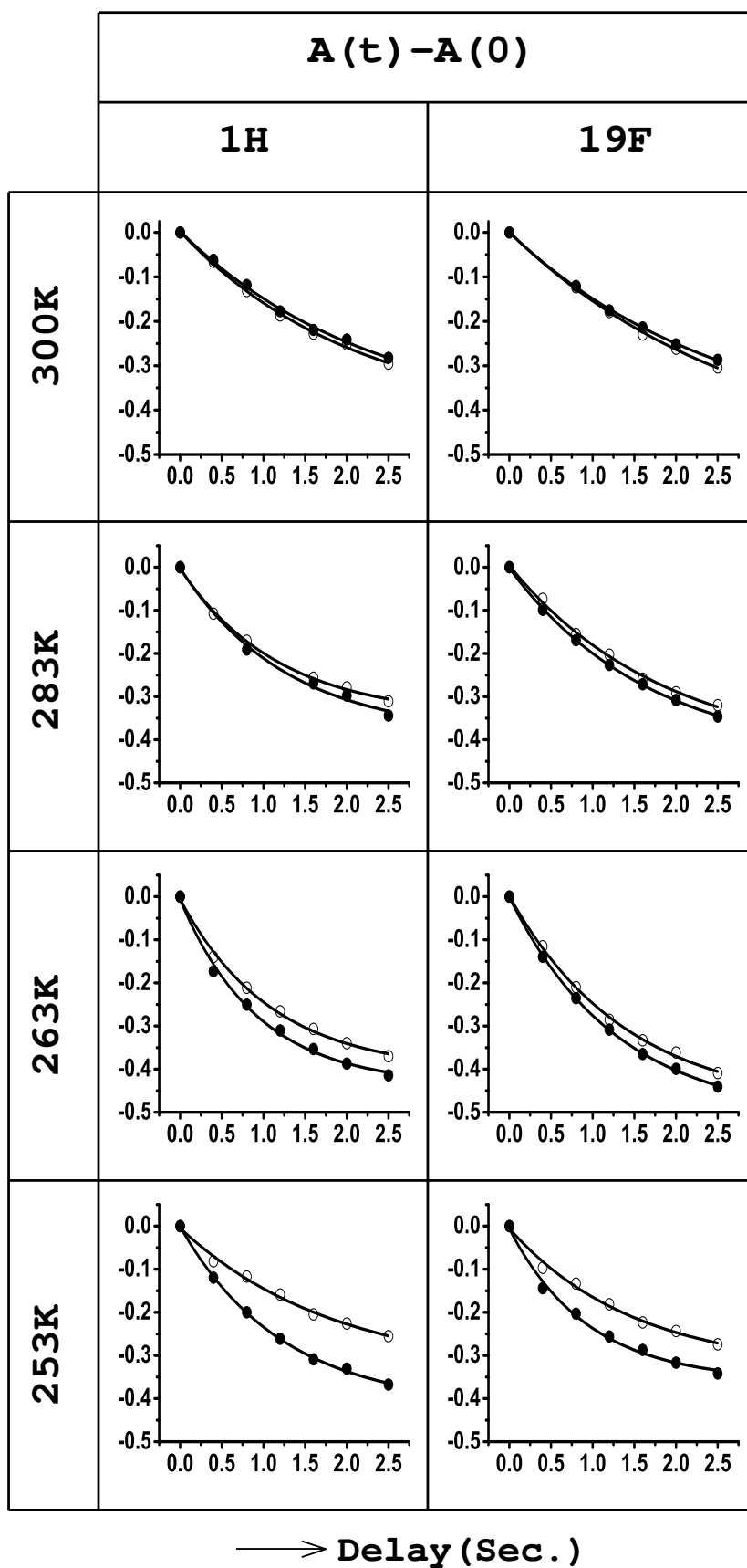


Figure 8:

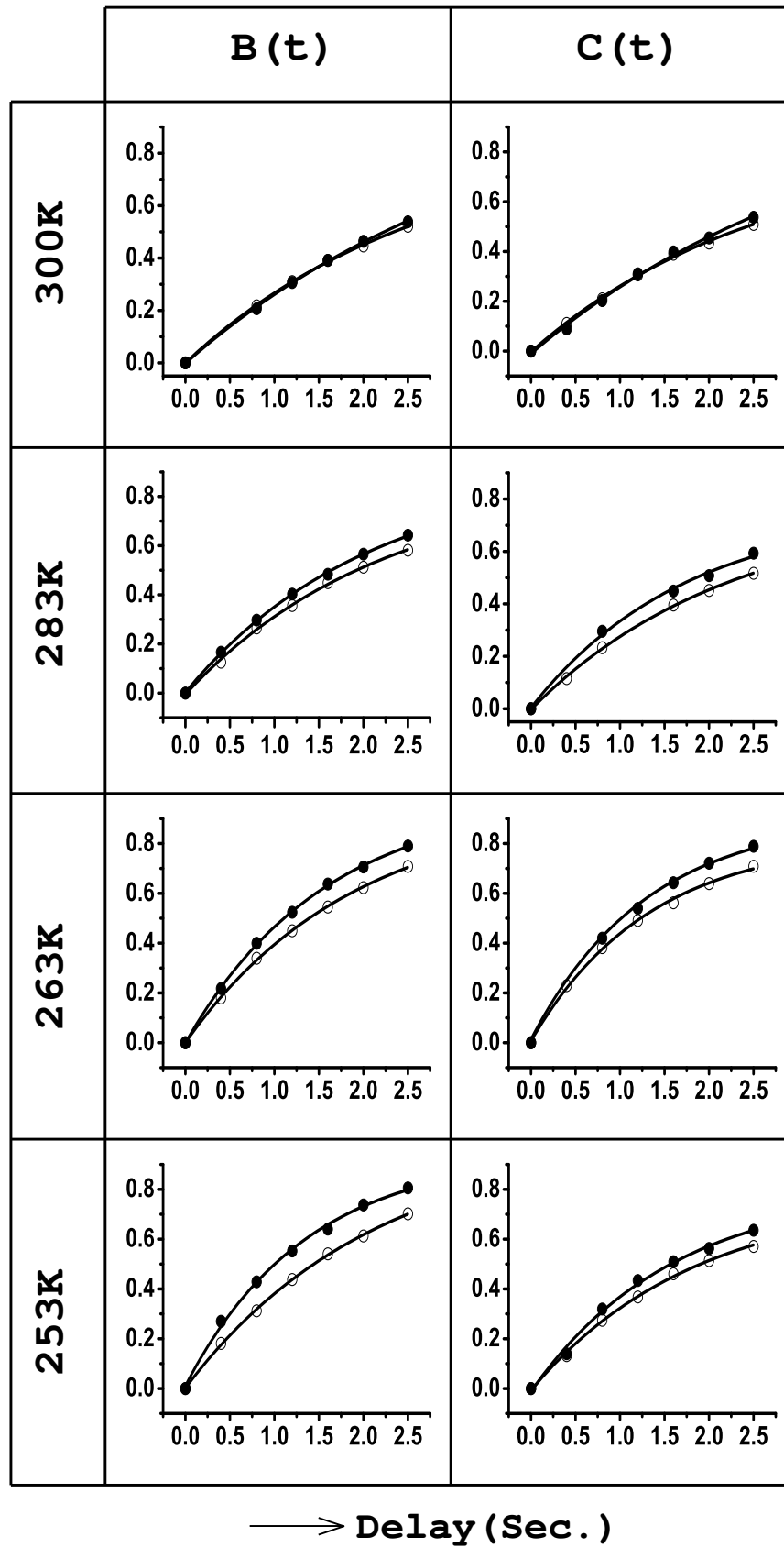


Figure 9: